

A CORRELATIVE STUDY BY ELECTRON AND LIGHT MICROSCOPY OF THE DEVELOPMENT OF TYPE 5 ADENOVIRUS

I. ELECTRON MICROSCOPY*

BY COUNCILMAN MORGAN, M.D., GABRIEL C. GODMAN, M.D.,
PETER M. BREITENFELD, Ph.D., AND HARRY M. ROSE, M.D.

*(From the Department of Microbiology, College of Physicians and Surgeons,
Columbia University, New York)*

PLATES 16 TO 32

(Received for publication, March 24, 1960)

Tissue cultures infected with adenoviruses contain intranuclear, Feulgen-positive crystals (1) which have been shown by correlative light and electron microscopic studies to be composed of viral particles (2). In addition, Feulgen-negative, protein crystals (3) devoid of recognizable virus (4) and viral antigen (5) are associated with infections by certain strains of type 5 adenovirus. This report, which is divided into two parts, describes additional observations on the mode of viral development. In the first, the electron microscope has been used to discern the structure of the viral particles and the morphologic details of the non-viral protein crystals, as well as to observe the cytologic changes that occur during cellular infection. In the second, the sequential stages of infection as seen in the cell by means of light microscopy are presented, the results of detailed histochemical studies are discussed, and the information gained by both electron and light microscopy is correlated in an attempt to delineate the manner in which the virus develops.

Materials and Methods

Two cell lines were employed, HeLa and HEp-2 (FJ), the latter originally derived from human laryngeal carcinoma by Dr. A. E. Moore. HeLa cells were grown in a medium consisting of lactalbumin hydrolysate (0.5 per cent), yeast extract (0.1 per cent), and dextrose (0.25 per cent) in Earle's balanced salt solution, and 20 per cent inactivated horse serum. Alternatively, Scherer's maintenance solution with 20 per cent horse serum was used. HEp-2 cells were grown in Eagle's basal medium with 10 or 20 per cent horse serum. For virus propagation, bottle-cultured cells were trypsinized and distributed into either plain tubes, 30,000 to 50,000 cells per tube, or into Leighton tubes, with a somewhat higher concentration of cells. Confluent monolayers were achieved in 3 to 5 days. Prior to virus inoculation the fluids were replaced with fresh medium.

* These studies were conducted under the auspices of the Commission on Influenza, Armed Forces Epidemiological Board and were supported in part by the Office of The Surgeon General, Department of the Army, Washington, D. C., and by a grant from The National Foundation.

Four strains of type 5 adenovirus were used, all having been kindly supplied by Dr. R. J. Huebner and Dr. W. P. Rowe. The strains were designated AD-75, 196 (Rowe), 50678, and 50681. Each had been passaged at least once in HeLa or HEp-2 cells before inoculation. Dilutions of virus for inoculation were made in the same medium present in the tubes to be inoculated, one part virus dilution (10^{-1} or 10^{-2}) being added to four parts culture fluid. The fluids in inoculated tubes were not subsequently changed, as marked cytopathic effects were regularly observed within 4 days after inoculation. At this time the cells were collected for fixation, their removal from the glass being effected either with trypsinization, or by scraping them off into a small volume of balanced salt solution. They were washed twice in balanced salt solution and centrifuged to form small pellets. Except as indicated, the pellets were fixed for 20 minutes at room temperature in buffered, 1 per cent osmium tetroxide, dehydrated in graded dilutions of ethyl alcohol, embedded in methacrylate, and sectioned as previously described (6). An RCA type EMU-2E electron microscope was used.

In view of the fact that no major morphologic differences were noted between the two cell lines employed, specific identification will not be made in describing the micrographs. Only cells infected with viral strain AD-75 are illustrated.

RESULTS

I. General Morphology of the Normal Nucleus.—

Fig. 1M¹ illustrates part of an uninfected cell. The nucleus contains fine reticular and granular material as well as three characteristic, dense nucleoli. The double nuclear membrane exhibits differing orientation, and hence definition, in the section. Those portions of the nucleus at the bottom and right margins, which appear to be separate from the main body of the nucleus, are undoubtedly lobes that join at a level removed from the plane of section. Traversing the upper left corner are the interdigitated processes of two contiguous cells.

II. General Morphology of the Infected Nucleus.—

In Fig. 2M, showing a portion of a cell from an infected tissue culture, no viral particles can be identified, although changes in the nucleus are evident. In the right half of the field several aggregates of fine reticular material, three of which are indicated by the letter *a*, can be distinguished from the somewhat more dense nucleoli (marked *n*) and less dense matrix. This matrix material will hereafter be referred to as nuclear substance. In addition, there are two dense, sharply circumscribed bodies (marked *b*). In Fig. 3M the reticular aggregates instead of being small and circumscribed are larger, more diffuse, and, particularly evident near the center of the field, interconnected, thus forming strands. There are three dense, irregularly contoured nucleoli. No virus is visible.

Fig. 4M illustrates a nucleus containing discrete, localized aggregates of reticulum. Although the reticulum is disposed in a manner similar to that shown in Fig. 2M, the nuclear substance is not as uniformly distributed. Translucent zones have become apparent, particularly at the periphery, and within them scattered viral particles (several of which are indicated by arrows) may be seen. Fig. 5M demonstrates the ap-

¹ The letter M, following the figure number, is used to denote the electron micrographs and, thus, facilitate reference to them in Paper II of this communication.

pearance of the same nucleus in a thinner section.² Owing to diminished superimposition, the density of the reticular aggregates is less, while their structure is more clearly delineated. Comparison of these two micrographs serves to emphasize the effect of section thickness on the over-all appearance of the nucleus. (Such differences must obviously be kept in mind when comparing electron micrographs and more particularly, as will subsequently become apparent, when comparing an electron micrograph with a photograph of a whole cell.)

In Fig. 6M the nuclear substance is unevenly distributed and there are scattered reticular aggregates resembling those shown in Fig. 5M. The opaque structure within the zone of diminished density to the right of two nucleoli near the top, when viewed at higher magnification (Fig. 7M), exhibits diffuse margins and contains parallel lines with the 400 Å spacing encountered in the non-viral protein crystals (4). In the adjacent matrix are scattered fibrils and granules. The nucleoli, partly visible at the left margin, have a characteristic granular appearance. Fig. 8M shows a nucleus containing scattered viral particles and areas of diminished density, two of which surround non-viral crystals (indicated by arrows). The lower crystal possesses diffuse margins, whereas the upper, although devoid of flat faces, is more sharply delineated. In the upper third of the nucleus are several small viral crystals partially enclosed by interconnected strands of reticular material, which exhibit greater density than the adjacent nuclear substance. The nucleus illustrated in Fig. 9M exhibits on the left a large zone of diminished density containing numerous scattered viral particles and a hexagonal, protein crystal. Two dense, sharply defined bodies with less opaque centers are indicated by arrows. In the central and right-hand portions of the field, strands of dense reticulum are closely approximated to crystals of virus. Examination of similar reticulum at higher magnification (Fig. 10M) reveals that it is composed of thin filaments and granules which are both more opaque and more closely approximated than those constituting the usual nuclear substance (designated *ns*). At the top and right of the picture is a zone of low density containing the type of fine granules and fibrils which were also apparent in Fig. 7M. This substance will be termed matrix hereafter. In addition to viral particles, which appear most numerous in the vicinity of the dense reticulum, there are opaque, irregularly shaped bodies (several of which are indicated by arrows). In Fig. 11M the virus tends to line the surface of the dense reticulum, whereas there is no concentration of virus at the margins of the remnants of nuclear substance (*ns*).

Fig. 12M illustrates a nucleus with a central mass of dense reticulum containing viral crystals and surrounded by nuclear substance. In the wide peripheral zone of matrix are numerous, scattered viral particles, an hexagonal crystal, and several oval, dense bodies (indicated by arrows). Just above and to the right of the crystal is a crescent-shaped nucleolus, which, at higher magnification (Fig. 13M), is seen to be composed of small granules. Figs. 14M and 15M, showing portions of other nucleoli at the same magnification, reveal the relatively large granules occasionally encountered. In Fig. 16M the matrix, containing scattered virus and protein crystals, is extensive,

² Sections of viral crystals can be shown, by superimposing transparent prints, to vary in thickness by a factor of 3, while still permitting high resolution micrographs to be obtained (7).

whereas the remnants of nuclear substance and the dense, reticulum (near the center and at the upper left) occupy relatively small areas. Scattered through the reticulum are irregularly shaped, homogeneous, opaque bodies resembling those illustrated in Fig. 10M. The crystals possess sharply defined, generally flat faces and are devoid of viral particles (with the possible exception of the crystal near the left border in the upper third).

In Fig. 17M the nuclear membrane is discontinuous and appears to be folded back on itself. The nuclear substance with a few viral particles is visible at the lower left. The upper third and right half of the field are occupied by cytoplasm containing scattered viral particles and components of the nucleus. The nucleolus (marked *n*) is evident, as are opaque granules (near the upper margin). The lamellae circumferentially arranged at the lower right appear at higher magnification (Fig. 18M) to be membranous components of the endoplasmic reticulum. The dense body with diffuse margins (indicated by an arrow) exhibits at higher magnification (Fig. 19M) a suggestion of the linear pattern encountered in the non-viral, protein crystals. Below the viral particles at the right the nuclear membrane has reduplicated, a phenomenon which is discussed elsewhere (8). Fig. 20M illustrates part of a nucleus with a discontinuous membrane, scattered viral particles, and a protein crystal, the margins of which (especially in the upper third) are poorly defined. At the top the cellular wall and adjacent cytoplasm are absent with the result that virus and nuclear matrix are contiguous to the extracellular space. Fig. 21M is composed of two micrographs showing a long protein crystal partially contained within a distorted, swollen nucleus. On the right in the mid-third are numerous viral crystals embedded in dense reticulum. At the top and bottom the nuclear membrane has disrupted.

III. Viral Structure.—

In view of differing reports concerning the morphology of purified virus (9-11) and in the light of a remarkable demonstration by "negative staining" with phosphotungstic acid of viral subunits arranged in the form of an icosahedron (12), it was decided to examine the effects of different methods of preservation on the appearance of intranuclear virus.

If sections of formalin-fixed tissue were exposed to fumes of osmium tetroxide before bombardment in the electron beam, the viral particles exhibited a clearly delineated peripheral membrane about 650 Å in diameter, enclosing a core of variable density averaging 600 Å in cross-section (Fig. 22M). Some particles (of which two are indicated by arrows in the figure) had flattened faces, although no consistent crystalline configuration was apparent. As shown in Fig. 23M, however, fixation in osmium tetroxide for 20 minutes followed by 1 per cent KMnO_4 (pH 7.2) for 30 minutes frequently resulted in profiles suggestive of an icosahedron. Although quick freezing³ caused severe distortion of cellular architecture, the viral crystals were generally well preserved. In Fig. 24M, for example, the crystalline array of intranuclear viral particles is evident. The center-

³ After freezing in isopentane at -180° , the cells were placed in absolute ethyl alcohol at -50° for 7 days (13). Following this the tissue was embedded in methacrylate and sectioned.

to-center spacing approximates 650 Å and in some areas (indicated by arrows) oval, peripheral, viral membranes are visible. A striking difference from the osmium-fixed preparations is the relatively uniform density of the central body.

IV. Structure of the Protein Crystals.—

Fig. 25M illustrates a nucleus containing seven protein crystals and scattered viral particles. The two lowermost crystals exhibit poorly defined faces. The large elongated crystal in the mid-third has fairly sharp lateral faces, but the ends appear indistinct. The patterns of density vary depending upon the orientation of the crystalline lattice with respect to the plane of section, as is illustrated in the next two pictures. Crystals cut perpendicular to the long axis (Fig. 26M) exhibit an array of dense points with an approximate spacing of 400 Å, whereas in longitudinal section, as shown by Fig. 27M, a linear pattern is encountered. In the upper half of the latter picture are two viral particles lying within the crystal. After formalin fixation the crystalline lattice cannot be visualized (Fig. 28M) unless the section is exposed to fumes of osmium tetroxide within a closed container before examination in the microscope (Fig. 29M).

V. Ring-Like Bodies.—

Infected nuclei not infrequently contained sharply circumscribed bodies which appeared either uniformly opaque or exhibited central areas of diminished density (see Figs. 2M, 9M, and 12M). Two characteristic bodies are illustrated in Fig. 30M. They have a dense peripheral zone and an interior composed of fine granules and fibrils. Neither shows any spatial orientation to the virus.

DISCUSSION

Different methods of preservation bring out different aspects of viral structure. Fixation in osmium tetroxide, for example, reveals an oval particle with a central core of variable density. The peripheral membrane is poorly preserved, but the center-to-center spacing of 650 Å in crystalline arrays testifies to the presence of some structure with this diameter. Formalin permits clear visualization of the dense peripheral membrane averaging 650 Å in diameter (Fig. 22M). Although angular faces were encountered in such preparations, a profile consistent with an icosahedron was rarely observed. Treatment of the section with osmium tetroxide fumes is not necessary for delineation of the membrane, but the osmium does seem to stabilize or stain components of viral structure. When intracellular virus is fixed in potassium permanganate alone or after immersion in osmium tetroxide a profile consistent with an icosahedron is not infrequently encountered (Fig. 23M). This finding is consistent with the report by Epstein (11) on the effects of potassium permanganate on purified pellets of virus. Since one would expect consistent orientation of the virus within a crystalline lattice, it

appears likely that the variation in shape, seen in Fig. 23M, does not reflect differences in orientation of the virus with respect to the plane of section. The subunits which make up the icosahedron found by Horne *et al.* (12) exhibit a center-to-center spacing of 70 Å. Since this molecular spacing can easily be resolved in sections, our inability to visualize the subunits must result either from their deficient preservation or inadequate contrast. Finally, quick freezing results in the appearance of a spherical particle with a relatively uniform central body. The foregoing observations reflect a variability in viral shape which appears to depend upon the procedure employed for preservation. Which of the methods currently in use most closely approximates the structure of hydrated virus is unknown.

Cross-sections of the nonviral crystals reveal an hexagonal array of dense points with a spacing of approximately 400 Å (Fig. 26M). As was noted above, these points are not visible after formalin fixation (Fig. 28M) unless the section is exposed to fumes of osmium tetroxide (Fig. 29M). The foregoing suggests that osmium tetroxide either stains a portion of the molecules (or groups of molecules) composing the crystalline array or renders them more stable to the electron beam in a manner analogous to that encountered in the case of certain cellular components (14). The possibility exists that the dense points represent intermolecular spaces which are infiltrated by osmium during fixation. Such a concept, however, is difficult to reconcile with the effect of osmic fumes on sections of formalin-fixed crystals. In sections longitudinal to the long axis of the crystal, a parallel array of lines is seen, presumably indicating that the end-to-end separation of the dense portions is so small as not to be resolved. A similar situation probably accounts for the lines observed in thin sections of insect polyhedral protein crystals (15). It should be noted, however, that in the latter instance the spacing (65 Å) is much closer. Depending upon the angle of sectioning, the patterns of density vary (see Figs. 16M and 25M). If the crystal shown in Fig. 26M were cut longitudinally on a plane not quite parallel to the face which traverses the lower right corner, the section, in passing from one level of the lattice to the next, would bring into view a new set of lines spaced half-way between the preceding set. Thus the lines would appear staggered, a phenomenon presumed to account for the staggered arrays indicated by arrows in Fig. 27M. Distortion of the crystal introduced during preparation of the specimen probably accounts for the variability of the effect in other parts of the field.

Histochemical studies reveal that the peripheral zones of low density (matrix) in the nucleus contain protein material which stains in the same manner as, though less intensely than, the crystals. It appears likely that during infection the amount of protein increases until a sufficient concentration is reached for crystallization to occur. Why this concentration is achieved in nuclei infected with type 5 adenovirus but not with the other types (1 to 7 and 9 to 11) that we have examined remains unclear. Moreover, even with type 5, only one (AD75) of the three strains employed produced crystals with any degree of regularity.

At early stages of infection the crystals exhibit diffuse margins (Fig. 7M). Subsequently the margins appear to become more clearly delineated (Fig. 9M), for in nuclei showing advanced changes straight, sharply defined crystalline faces are the rule (Figs. 12M and 16M). These observations suggest that during the process of crystallization large numbers of molecules move relatively slowly from a state of random orientation into a crystalline array, the region of transition being signified at the periphery of the crystals by a diffuse zone where opacity to the electron beam differs from the nuclear matrix but no lattice is visible. Not infrequently crystals sectioned in a plane parallel to their long axis exhibit sharply defined sides and diffuse ends (Fig. 25M), an appearance consistent with the concept that crystallization is occurring mainly at the ends in such a manner as to produce the elongated forms repeatedly found. How adjacent viral particles are so often excluded from incorporation into the crystals and what basic difference distinguishes crystallization in this instance from the intranuclear crystallization of insect polyhedral protein, wherein numerous viral particles are enclosed (16, 17), are not known, but it may be noteworthy in this connection that close examination of fields, such as the one illustrated by Fig. 25M, rarely discloses viral particles in contact with the crystalline matrix. Electron micrographs of nuclei infected with a polyhedral virus (17), on the other hand, show the membrane of the viral rods apparently contiguous to the crystalline protein. If, in the former instance, the transition of protein molecules from random orientation into crystalline array occurs slowly, there might be present at the periphery of the crystal a wide zone of concentrated protein. These molecules, closely packed but arranged at random, would tend to displace the majority of viral particles and crystallization would thus proceed with exclusion of most of the virus. In the case of the polyhedral insect viruses, however, the process of crystallization may take place rapidly with the result that the zone of transition from random orientation to crystalline array would be very narrow and the clusters of viral rods, even though relatively large would become trapped within advancing crystalline matrix before displacement could occur.

With rupture of the nuclear membrane and release of virus, the crystals undergo dissolution, the margins becoming diffuse and the crystalline pattern appearing indistinct (Fig. 19M). Dissolution seems to be rapid, since crystals are rarely found in the cytoplasm. Crystallization and dissolution produce a similar appearance and, hence, the inference as to which process is taking place must be based upon whether the host cell is in an early or late stage of infection.

SUMMARY

Stages in the nuclear changes consequent to infection with type 5 adenovirus are shown and described. Viral development seems to be confined to the nucleus where characteristic particles are found. The shape of the intracellular virus depends upon the method of preservation employed, appearing spherical after osmium tetroxide or freezing-substitution, occasionally exhibiting angulated

faces after formalin and often assuming an hexagonal profile after potassium permanganate. The non-viral crystals are encountered in zones of low density, and it is suggested that crystallization results from the accumulation of protein in these areas. An hypothesis is presented to explain why these crystals, in contrast to the insect polyhedra, contain few viral particles.

BIBLIOGRAPHY

1. Boyer, G. S., Leuchtenberger, C., and Ginsberg, H. S., Cytological and cytochemical studies of HeLa cells infected with adenoviruses, *J. Exp. Med.*, 1957, **105**, 195.
2. Bloch, D. P., Morgan, C., Godman, G. C., Howe, C., and Rose, H. M., A correlated histochemical and electron microscopic study of the intranuclear crystalline aggregates of adenovirus (RI-APC virus) in HeLa cells, *J. Biophysic. and Biochem. Cytol.*, 1957, **3**, 1.
3. Leuchtenberger, C., and Boyer, G. S., The occurrence of intranuclear crystals in living HeLa cells infected with adenoviruses, *J. Biophysic. and Biochem. Cytol.*, 1957, **3**, 323.
4. Morgan, C., Godman, G. C., Rose, H. M., Howe, C., and Huang, J. S., Electron microscopic and histochemical studies of an unusual crystalline protein occurring in cells infected by type 5 adenovirus, *J. Biophysic. and Biochem. Cytol.*, 1957, **3**, 505.
5. Boyer, G. S., Denny, F. W., and Ginsberg, H. S., The sequential cellular changes produced by types 5 and 7 adenoviruses in HeLa cells and in human amniotic cells. Cytological studies aided by fluorescein-labelled antibody, *J. Exp. Med.*, 1959, **110**, 827.
6. Morgan, C., Howe, C., Rose, H. M., and Moore, D. H., Structure and development of viruses observed in the electron microscope. IV. Viruses of the RI-APC group, *J. Biophysic. and Biochem. Cytol.*, 1956, **2**, 351.
7. Morgan, C., Rose, H. M., Holden, M., and Jones, E. P., Electron microscopic observations on the development of herpes simplex virus, *J. Exp. Med.*, 1959, **110**, 643.
8. Gregg, M., and Morgan, C., Reduplication of nuclear membranes in HeLa cells infected with adenovirus, *J. Biophysic. and Biochem. Cytol.*, 1959, **6**, 539.
9. Valentine, R. C., and Hopper, P. K., Polyhedral shape of adenovirus particles as shown by electron microscopy, *Nature*, 1957, **180**, 928.
10. Tousimis, A. J., and Hilleman, M. R., Electron microscopy of type 5 adenovirus strain RI-67, *Virology*, 1957, **4**, 499.
11. Epstein M. A., Observations on the fine structure of type 5 adenovirus, *J. Biophysic. and Biochem. Cytol.*, 1959, **6**, 523.
12. Horne, R. W., Brenner, S., Waterson, A. P., and Wildy, P., The icosahedral form of adenovirus, *J. Mol. Biol.*, 1959, **1**, 84.
13. Deitch, A. D., and Godman, G. C., The application of a freezing-substitution method of fixation to tissue culture preparations, *Anat. Rec.*, 1955, **123**, 1.
14. Morgan, C., Moore, D. H., and Rose, H. M., Some effects of the microtome knife and electron beam on methacrylate-embedded thin sections, *J. Biophysic. and Biochem. Cytol.*, 1956, **2**, 21.

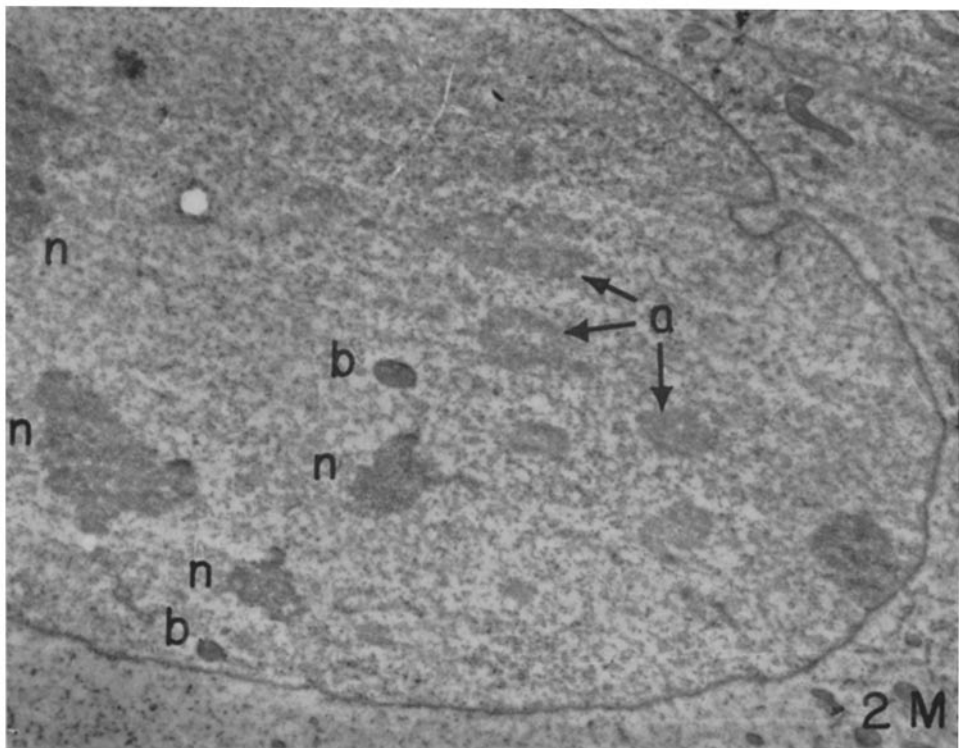
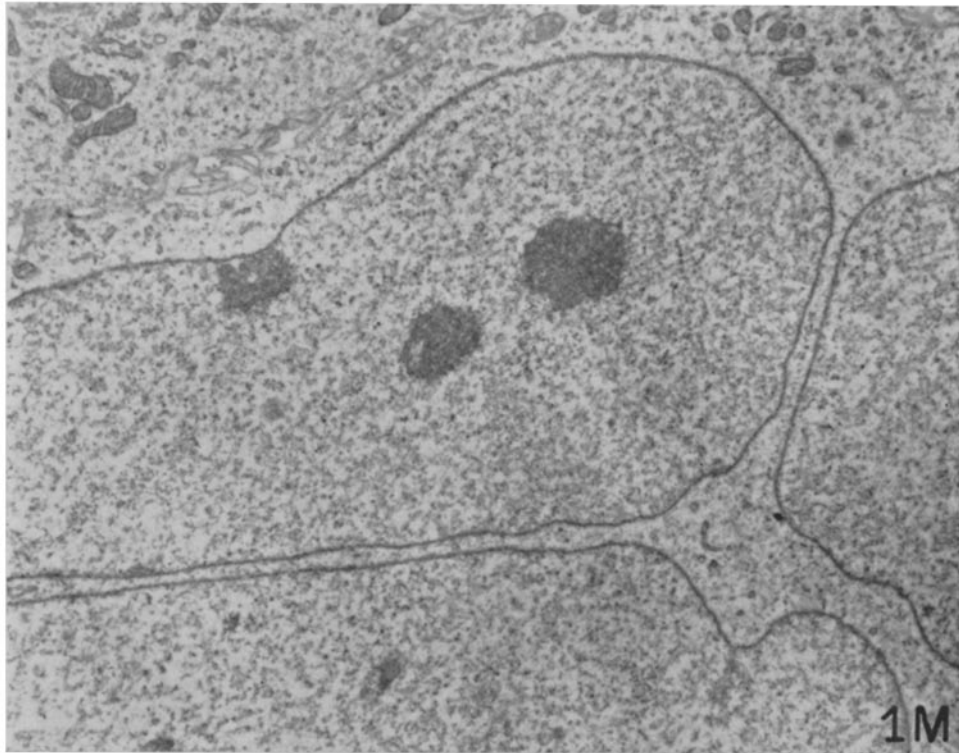
15. Morgan, C., Bergold, G. H., Moore, D. H., and Rose, H. M., The macromolecular paracrystalline lattice of insect viral polyhedral bodies demonstrated in ultra-thin sections examined in the electron microscope, *J. Biophysic. and Biochem. Cytol.*, 1955, **1**, 187.
16. Smith, K. M., Intranuclear changes in the polyhedrosis of *Tipula paludosa* (Diptera), *Nature*, 1955, **176**, 255.
17. Day, M. F., Farrant, J. L., and Potter, C., The structure and development of a polyhedral virus affecting the moth larva, *Pterolocera amplicornis*, *J. Ultrastruct. Research*, 1958, **2**, 227.

EXPLANATION OF PLATES

PLATE 16

FIG. 1M. A nucleus from an uninfected tissue culture. Three nucleoli are visible. Those portions of nucleus at the right and lower margins probably connect with the main body at a level removed from the plane of section. $\times 9,600$.

FIG. 2M. Part of a nucleus from an infected tissue culture. On the left are four dense nucleoli (*n*). On the right appear reticular aggregates, three of which are indicated by the letter *a*. Two dense, sharply defined, oval bodies are marked *b*. $\times 8,000$.



(Morgan *et al.*: Development of type 5 adenovirus. I)

PLATE 17

FIG. 3M. A nucleus with three nucleoli and aggregates of reticular material. Near the center of the field the aggregates interconnect, forming trabeculae. $\times 13,000$.

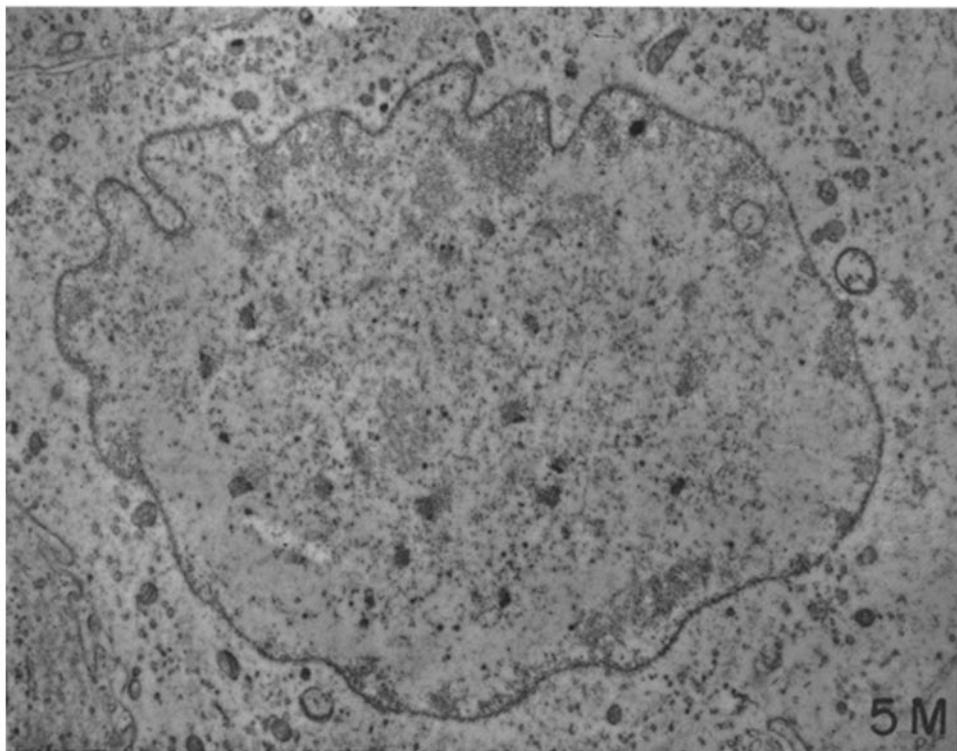
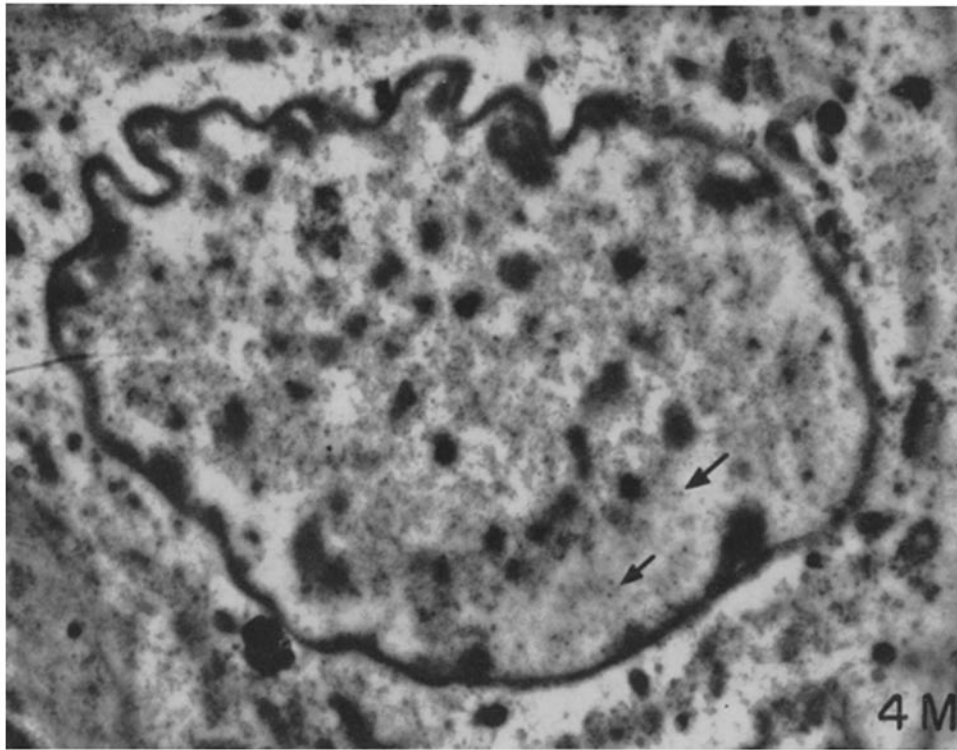


(Morgan *et al.*: Development of type 5 adenovirus. I)

PLATE 18

FIG. 4M. A nucleus with discrete aggregates of reticulum and peripheral zones of diminished density containing scattered viral particles (arrows). $\times 11,000$.

FIG. 5M. The same nucleus as it appears in a thinner section. $\times 11,000$

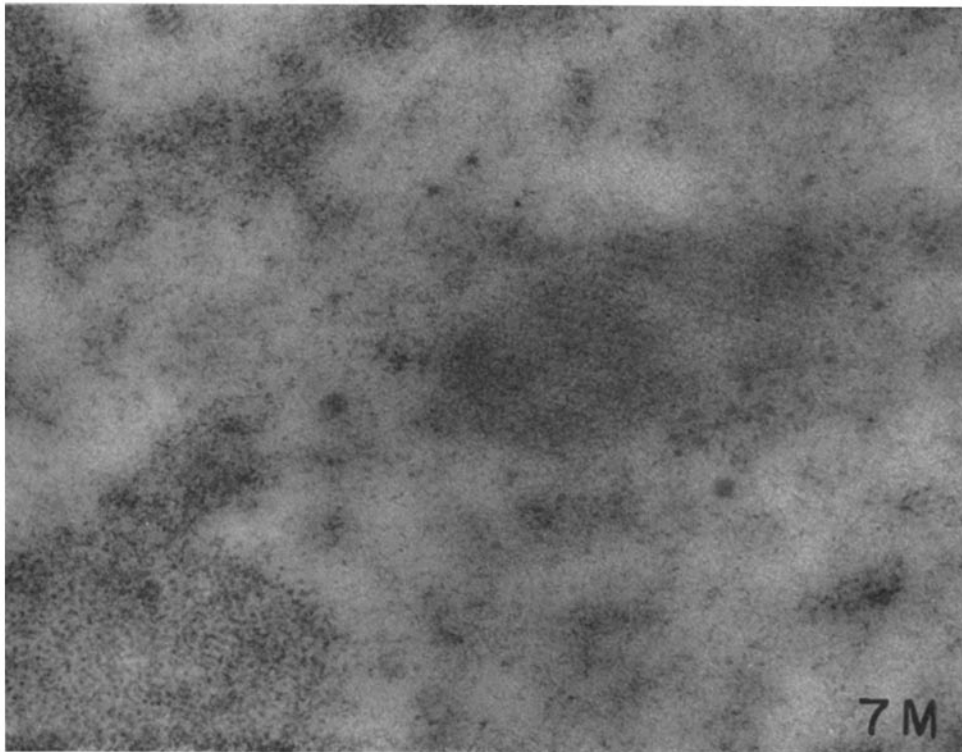
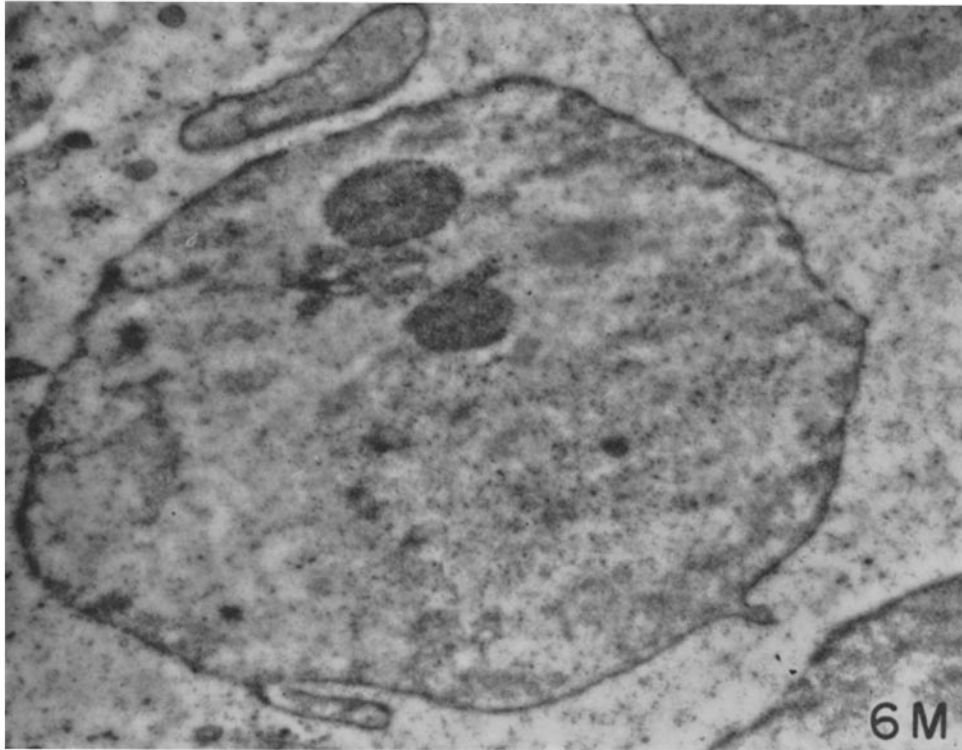


(Morgan *et al.*: Development of type 5 adenovirus. I)

PLATE 19

FIG. 6M. A nucleus showing scattered reticular aggregates. To the right of the two nucleoli is a zone of diminished density surrounding a dense, poorly defined body. $\times 11,000$.

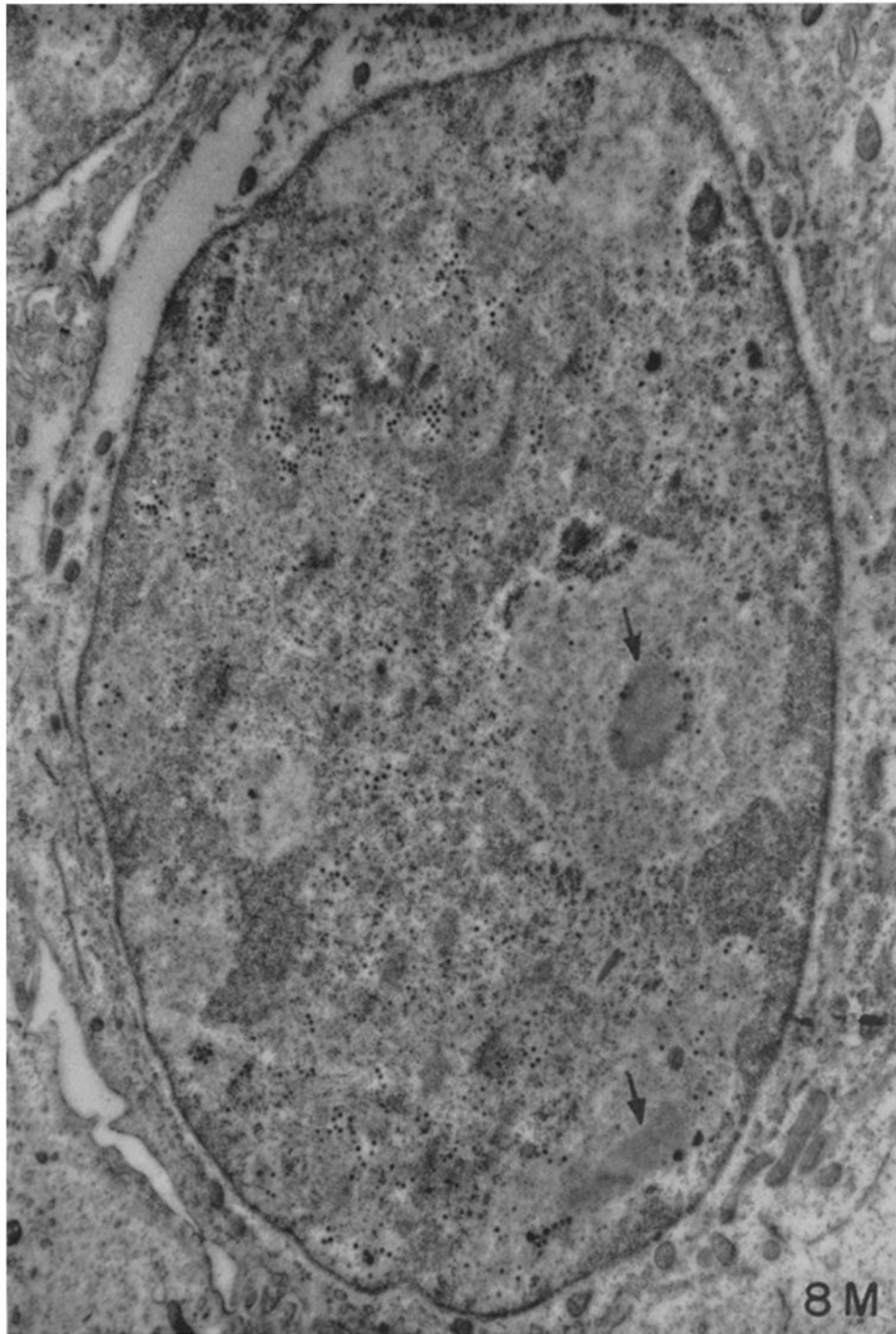
FIG. 7M. Part of the preceding figure at higher magnification. The dense body exhibits diffuse margins and contains dark, parallel lines spaced at 400 A. The surrounding matrix contains filaments and granules. $\times 54,000$.



(Morgan *et al.*: Development of type 5 adenovirus. I)

PLATE 20

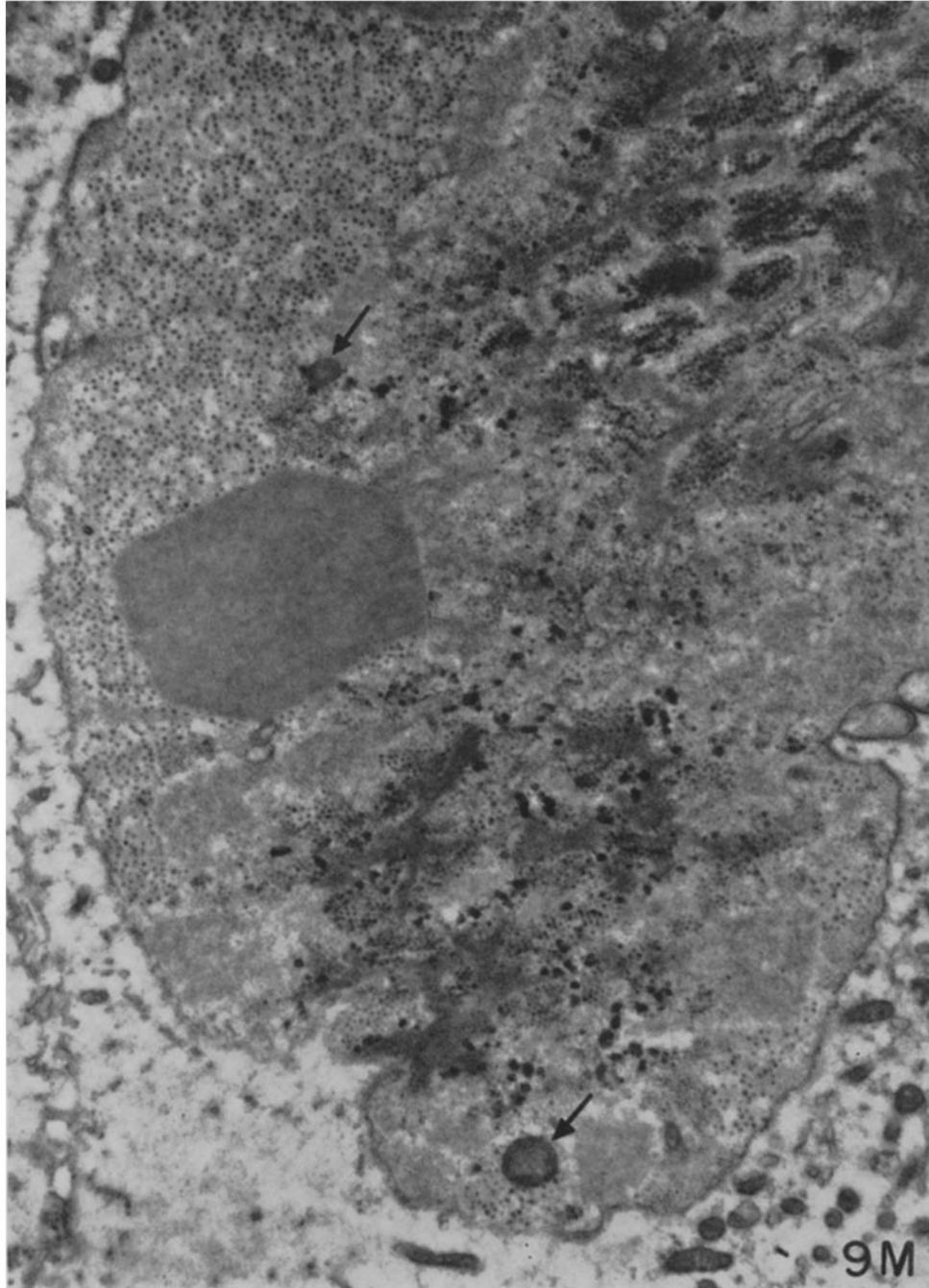
FIG. 8M. Two non-viral crystals (arrows) within a matrix of low density. There are scattered viral particles as well as small viral crystals (upper portion of the field).
× 13,000.



(Morgan *et al.*: Development of type 5 adenovirus. I)

PLATE 21

FIG. 9M. A hexagonal crystal in a nucleus containing a large amount of virus. Numerous viral crystals are closely approximated to dense reticular aggregates. Two ring-shaped bodies (arrows) are visible. $\times 12,500$.

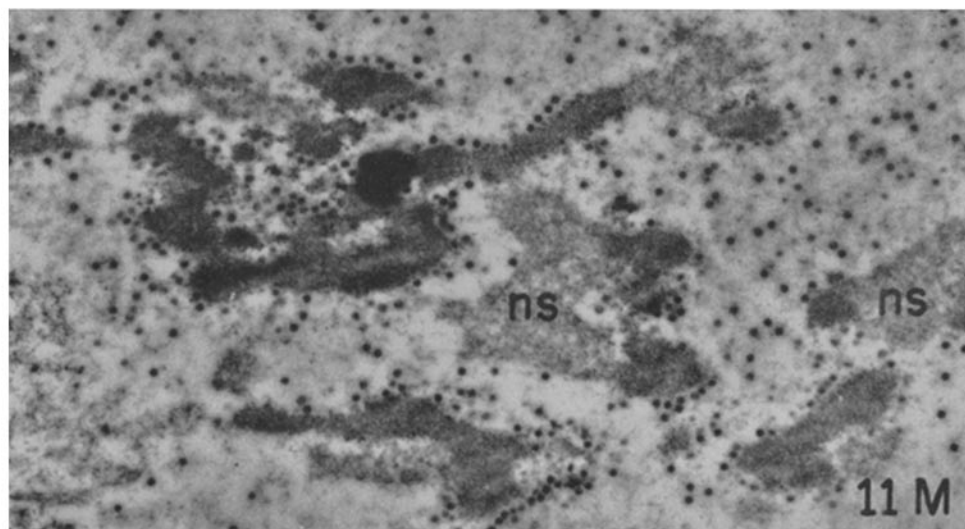
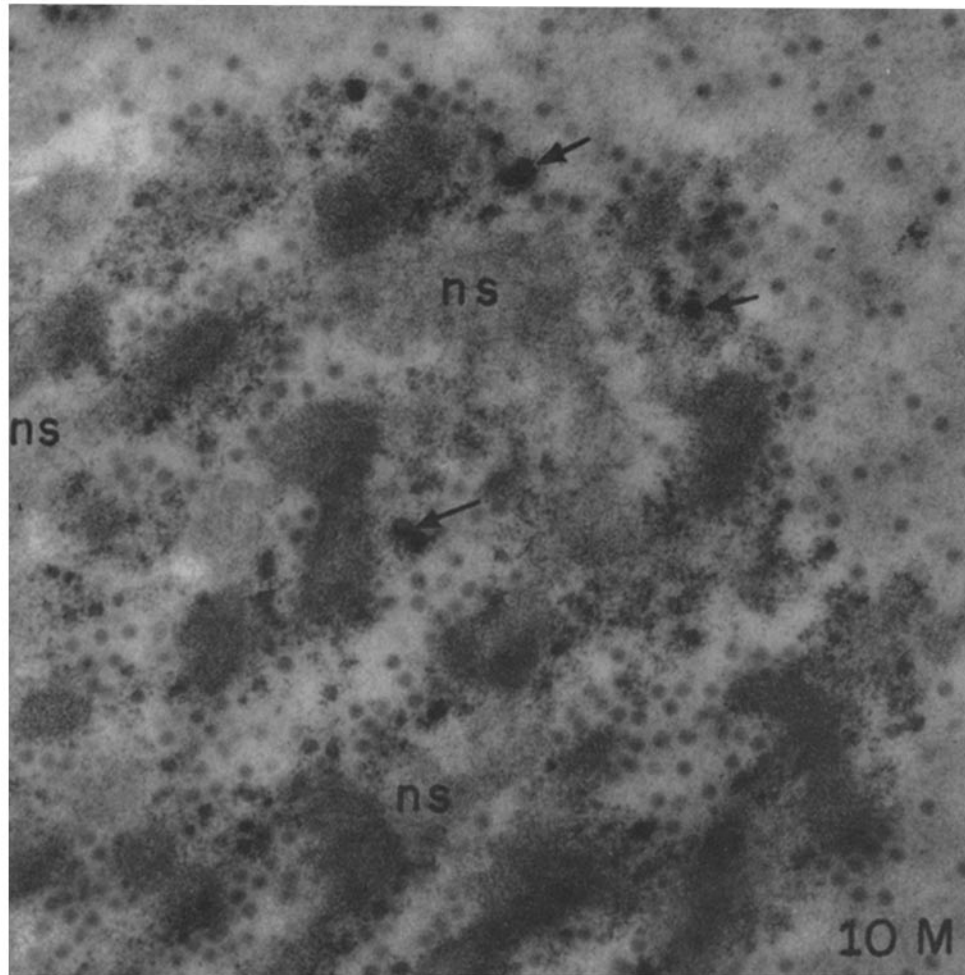


(Morgan *et al.*: Development of type 5 adenovirus. I)

PLATE 22

FIG. 10M. Viral particles between remnants of nuclear substance (*ns*) and dense reticulum. Opaque, oval structures are indicated by the arrows. $\times 40,000$.

FIG. 11M. Viral particles lining the surface of the dense reticulum and scattered at random in the matrix. $\times 17,000$.



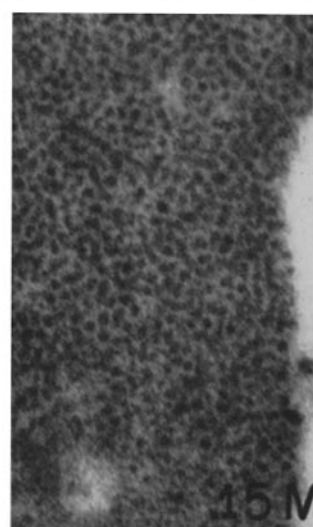
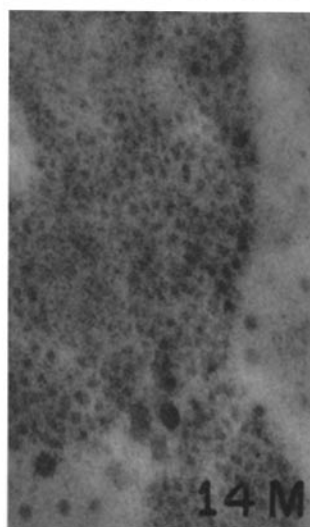
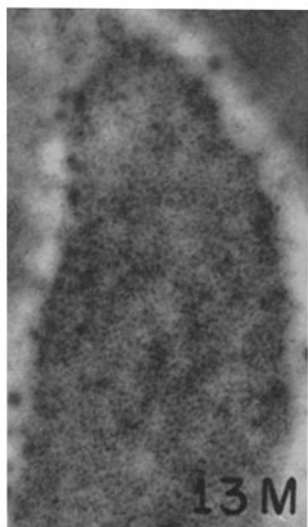
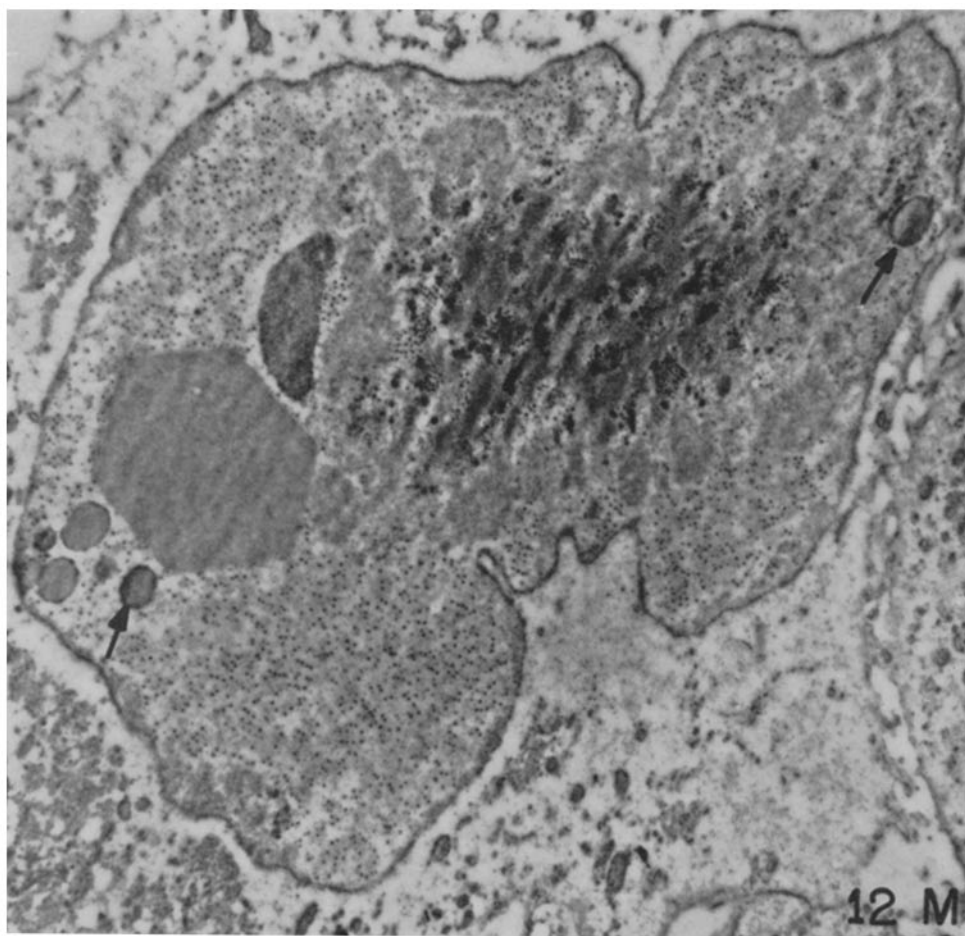
(Morgan *et al.*: Development of type 5 adenovirus. I)

PLATE 23

FIG. 12M. A nucleus with a large, central aggregate of reticulum and viral crystals and with a peripheral zone containing virus, an hexagonal crystal, a crescent-shaped nucleolus, and several oval, sharply defined bodies (arrows). $\times 8,000$.

FIG. 13M. The granules composing the nucleolus in Fig. 12M, as seen at higher magnification. $\times 37,000$.

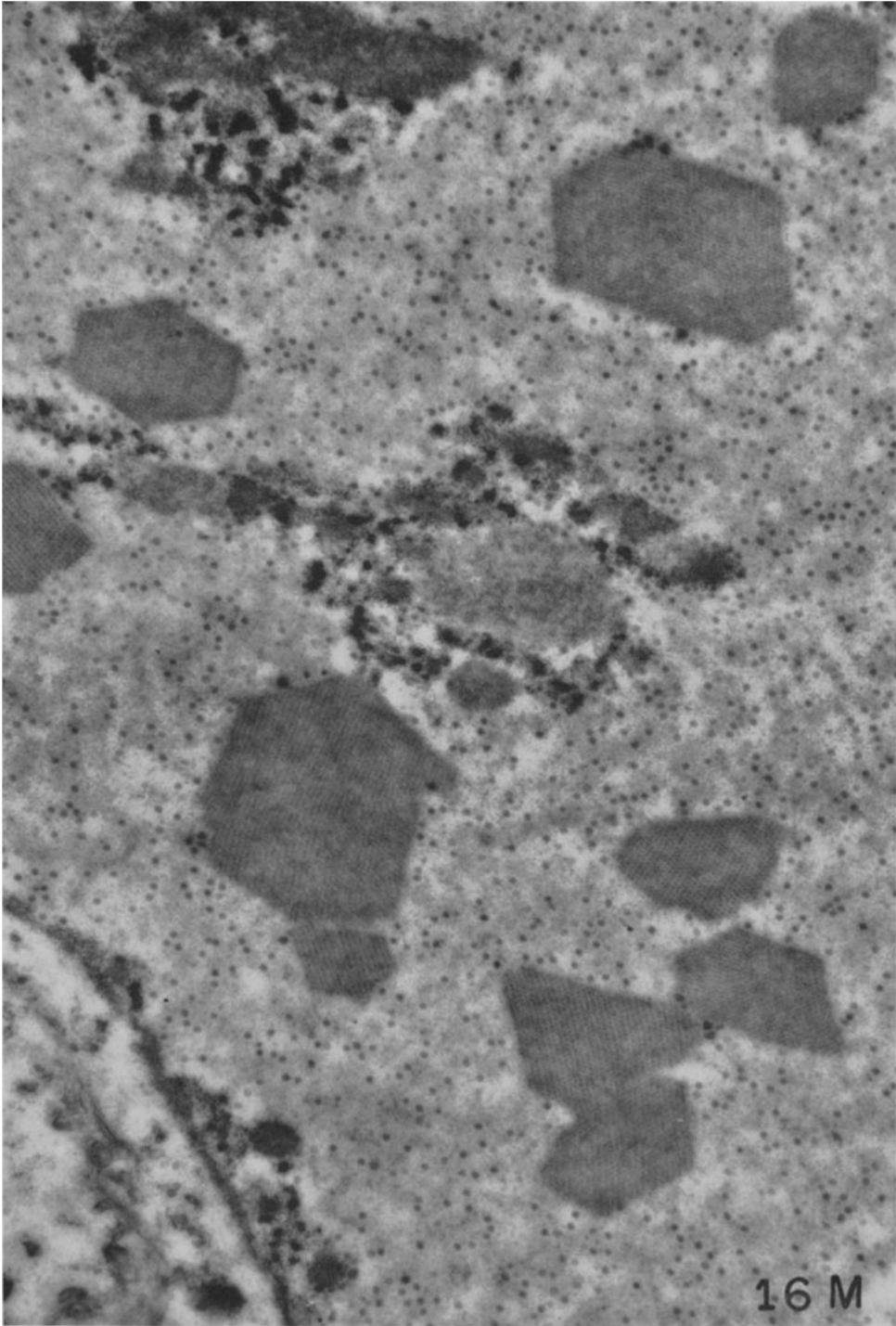
FIGS. 14M and 15M. Portions of other nucleoli, which exhibit a striking granular appearance. $\times 37,000$.



(Morgan *et al.*: Development of type 5 adenovirus. I)

PLATE 24

FIG. 16M. Non-viral crystals with sharp, flat faces. The matrix also contains scattered virus as well as clustered fragments of nuclear substance, dense reticulum, and opaque material. $\times 20,000$.



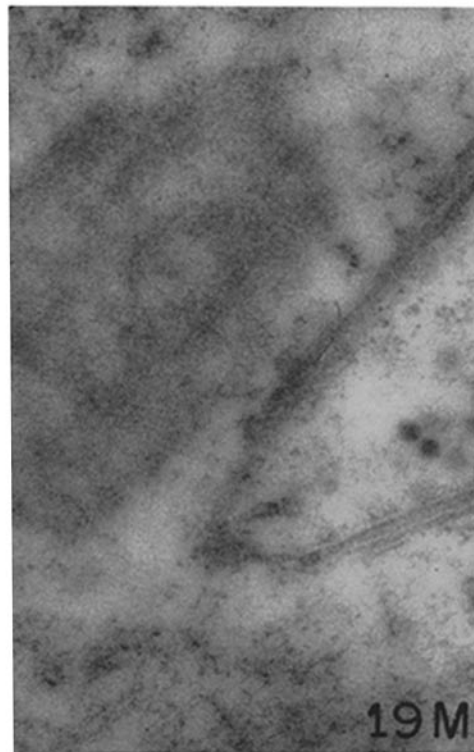
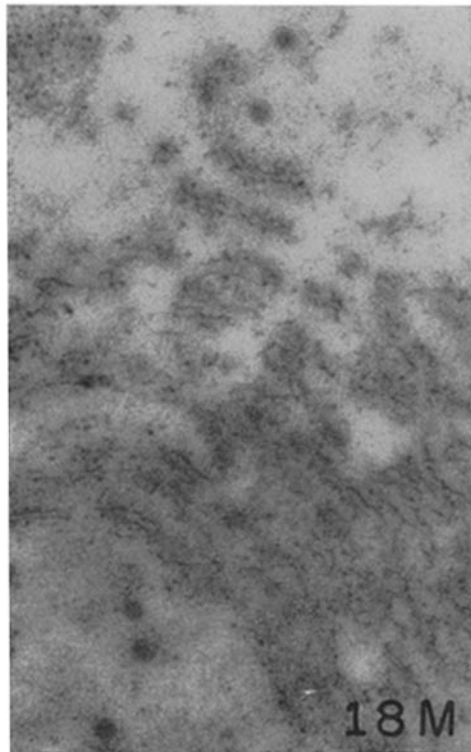
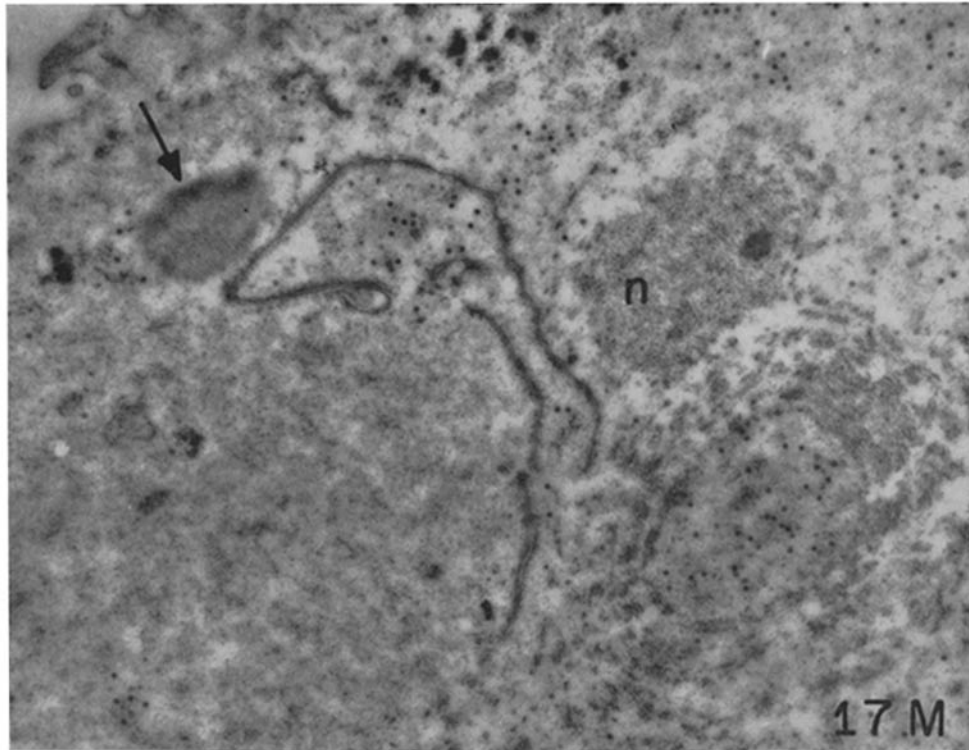
(Morgan *et al.*: Development of type 5 adenovirus. I)

PLATE 25

FIG. 17M. A cell with a disrupted nucleus. The discontinuous nuclear membrane is visible in the central portion of the field. Nuclear material occupies the lower left. Within the cytoplasm at the top and in the right half are scattered viral particles, a nucleolus (*n*), and a non-viral crystal (arrow). $\times 13,000$.

FIG. 18M. Part of the concentric lamellae below the nucleolus viewed at higher magnification in a different section. $\times 51,000$.

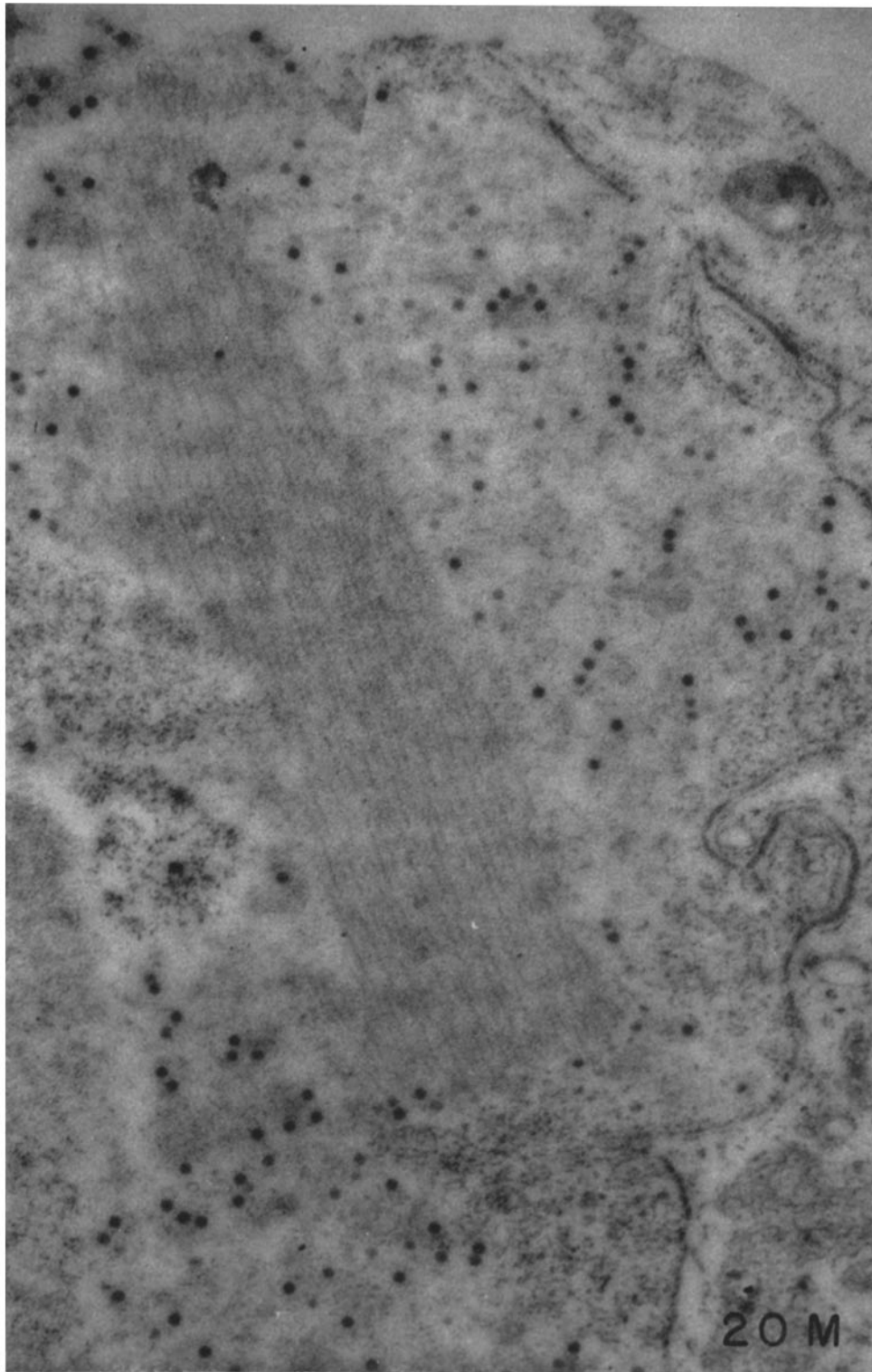
FIG. 19M. The non-viral crystal showing diffuse margins and a poorly preserved linear pattern. $\times 51,000$.



(Morgan *et al.*: Development of type 5 adenovirus. I)

PLATE 26

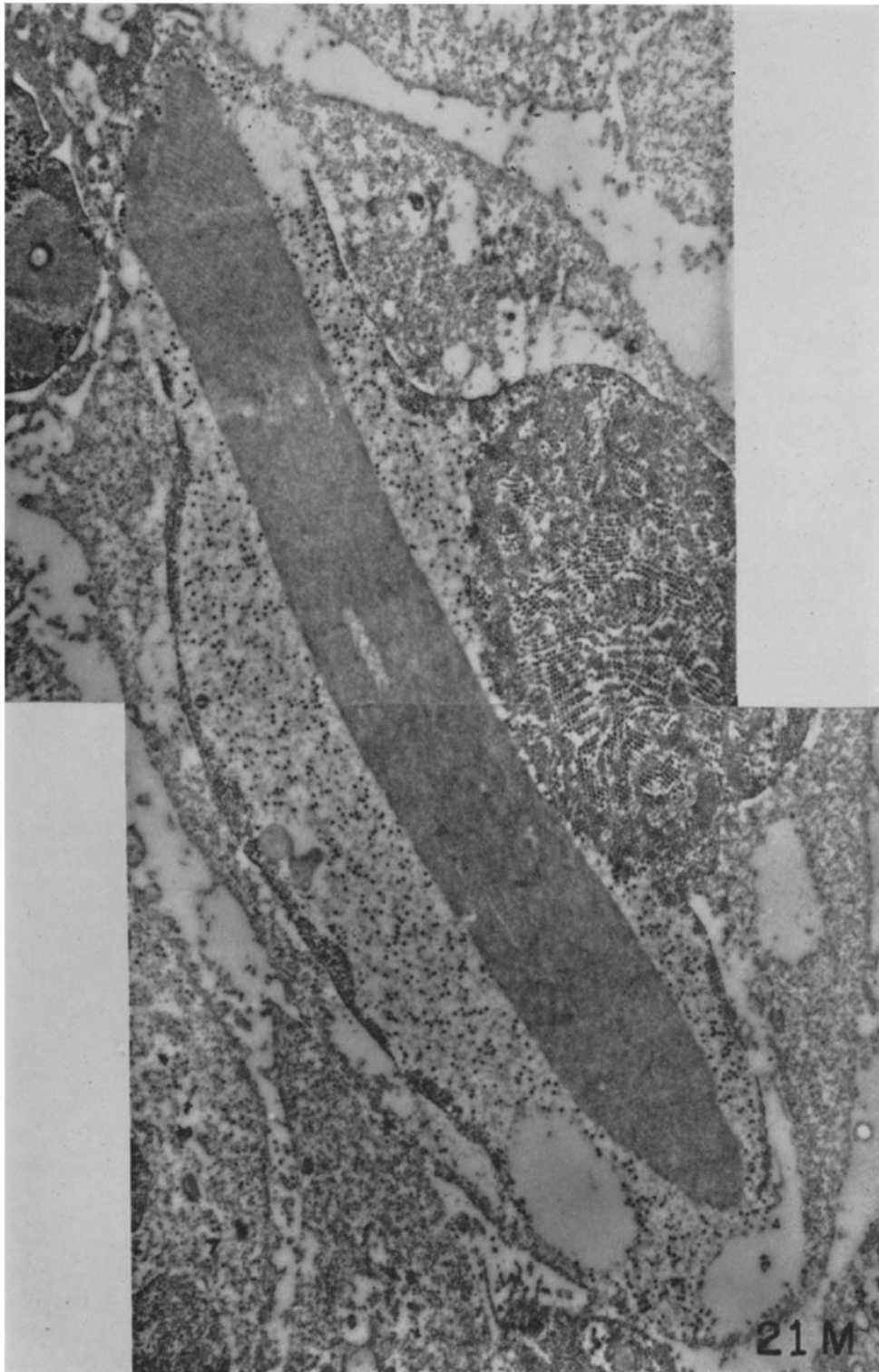
FIG. 20M. A nucleus containing scattered virus and a protein crystal with diffuse margins. The nuclear membrane is discontinuous and at the top the cytoplasm is absent, thus bringing nuclear contents into contact with the extracellular space. Viral particles appear to be in process of release. $\times 26,000$.



(Morgan *et al.*: Development of type 5 adenovirus. I)

PLATE 27

FIG. 21M. Two micrographs showing an elongated protein crystal lying within a distorted, ruptured nucleus. $\times 7,000$.

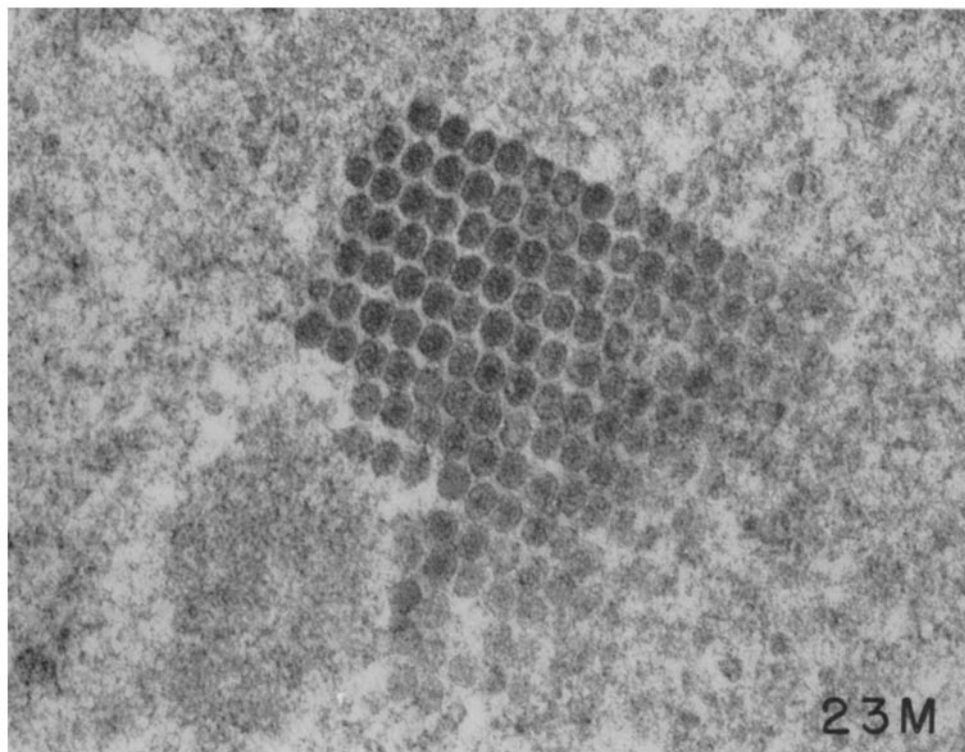
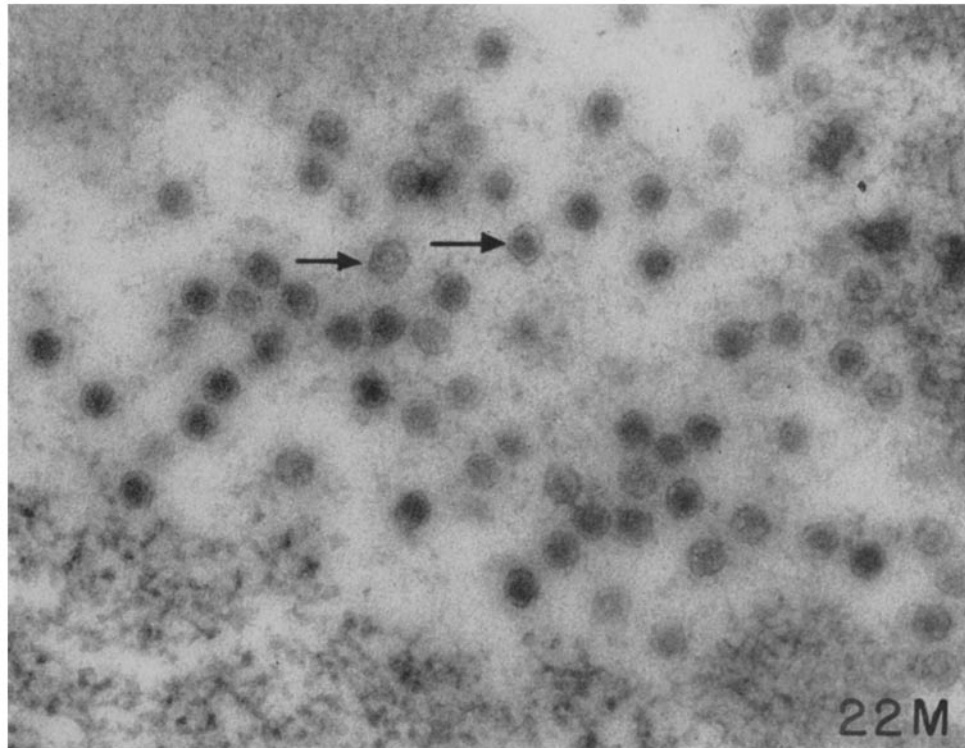


(Morgan *et al.*: Development of type 5 adenovirus. I)

PLATE 28

FIG. 22M. The appearance of virus after formalin fixation of the tissue and treatment of the section with fumes of osmium tetroxide. The arrows indicate two particles with flattened faces. $\times 80,000$.

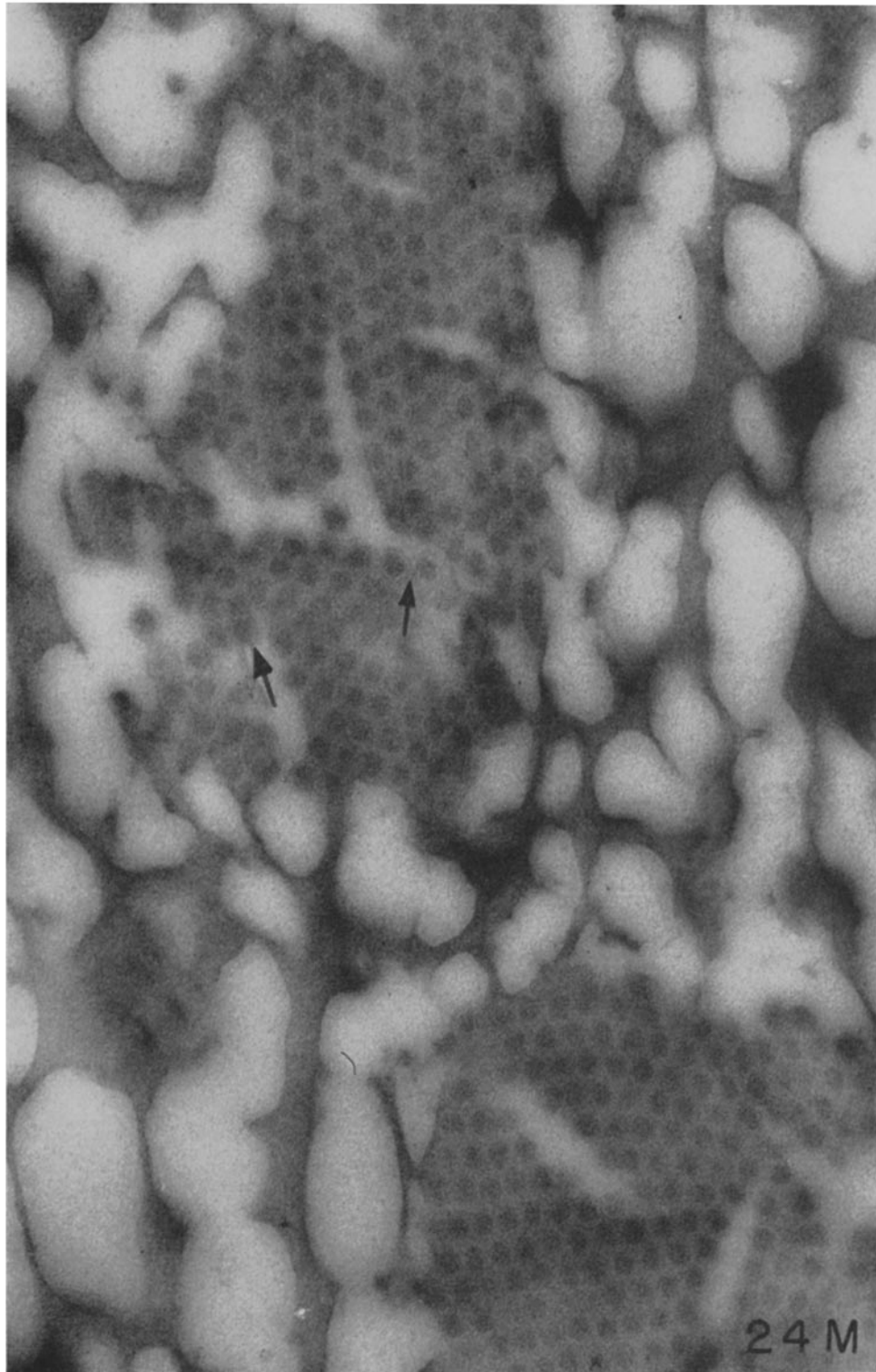
FIG. 23M. A viral crystal after fixation of the cell in osmium tetroxide followed by immersion in potassium permanganate. Several particles exhibit an hexagonal contour. $\times 80,000$.



(Morgan *et al.*: Development of type 5 adenovirus. I)

PLATE 29

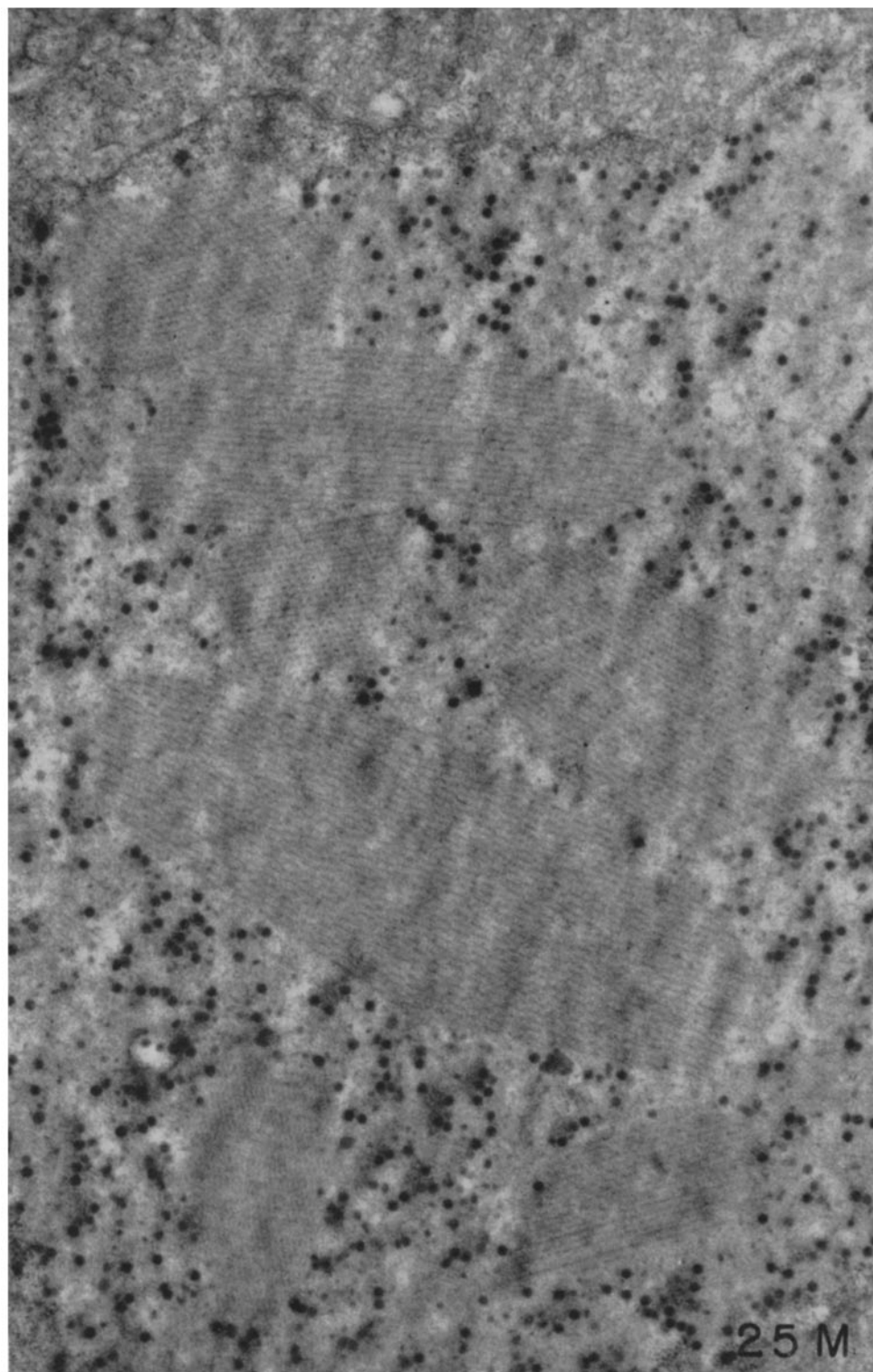
FIG. 24M. Part of a nucleus after treatment by freezing-substitution. The nuclear matrix is distorted, but the two viral crystals are clearly recognizable despite the presence of linear clefts. The virus appears spherical and the central core is relatively uniform in density. The arrows indicate areas where peripheral viral membranes are evident. This section was exposed to fumes of osmium tetroxide before examination. $\times 78,000$.



(Morgan *et al.*: Development of type 5 adenovirus. I)

PLATE 30

FIG. 25M. Protein crystals cut at differing angles. Few viral particles are contiguous to the crystalline matrix. $\times 26,000$.

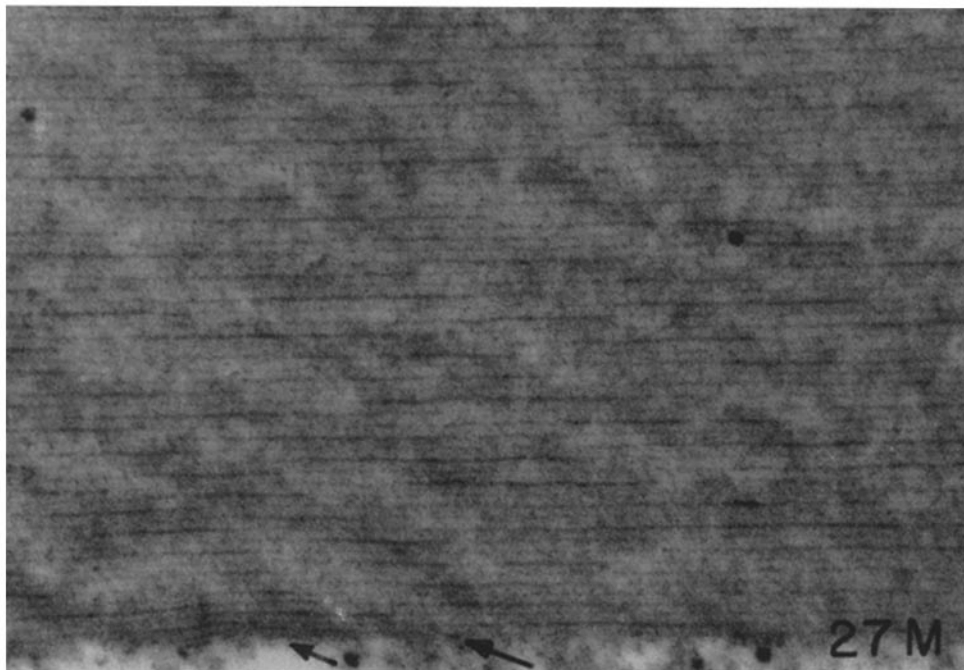
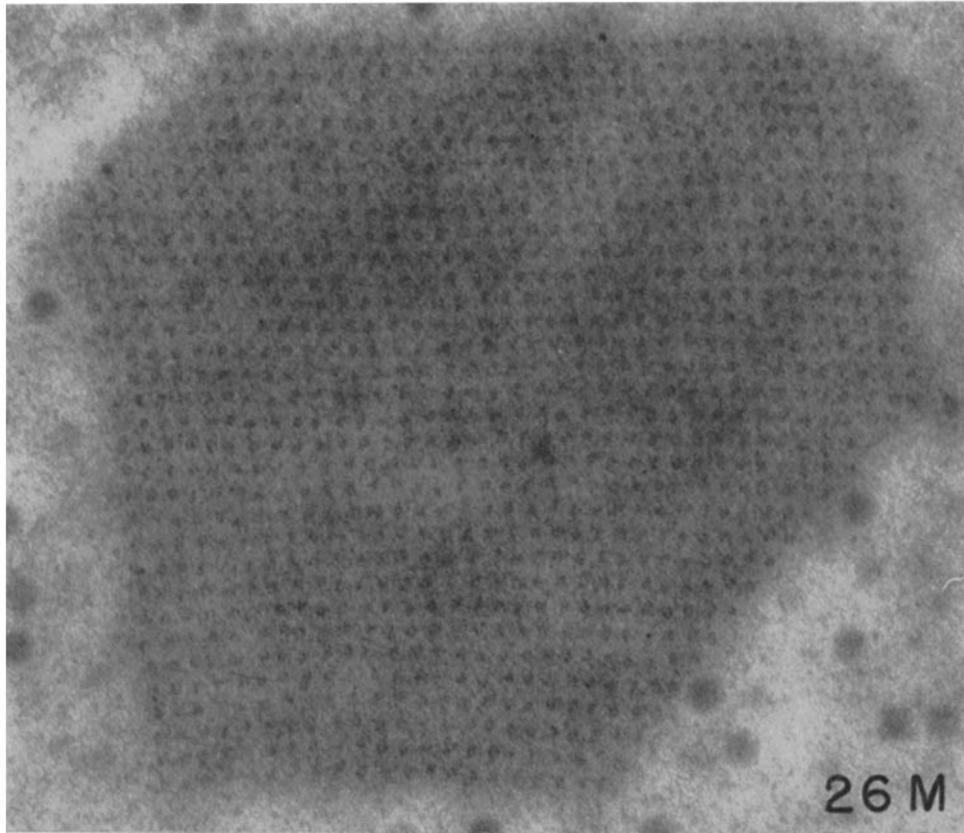


(Morgan *et al.*: Development of type 5 adenovirus. I)

PLATE 31

FIG. 26M. An hexagonal crystal with relatively sharp, flat faces. The section is perpendicular to the long axis and points of density are visible in crystalline array. The spacing averages 400 Å. $\times 80,000$.

FIG. 27M. A crystal cut nearly perpendicular to the long axis. The dense lines present a "staggered" appearance in several areas. $\times 37,000$.



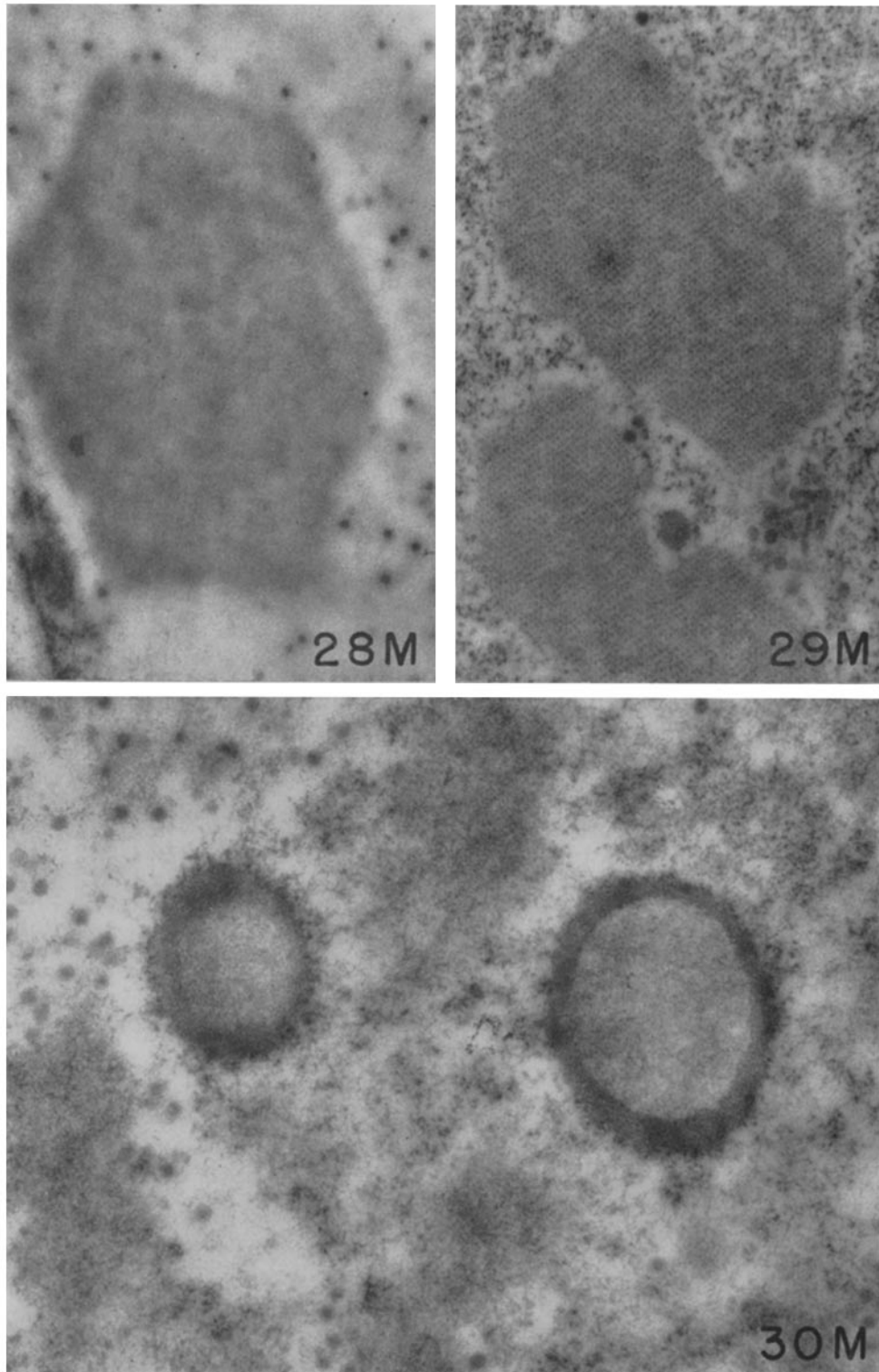
(Morgan *et al.*: Development of type 5 adenovirus. I)

PLATE 32

FIG. 28M. A crystal in cross-section after formalin fixation. No structure is evident. $\times 26,000$.

FIG. 29M. Two crystals fixed in formalin. This section was exposed to fumes of osmium tetroxide before examination. The crystalline array is visible. $\times 26,000$.

FIG. 30M. Two ring-like bodies composed of a dense reticular membrane enclosing granules and filaments. $\times 37,000$.



(Morgan *et al.*: Development of type 5 adenovirus. I)